

RESEARCH ARTICLE

10.1029/2018JC013824

Key Points:

- The 3-D structure, dynamics, and variability of the Subtropical Shelf Front were characterized for the first time
- Our main discovery is that the offshore detrainment of Subantarctic Shelf Waters occurs mainly near the Brazil-Malvinas Confluence
- This offshore detrainment might be affecting the population abundances of fishing resources in Argentina, Uruguay, and Southern Brazil

Correspondence to:

B. C. Franco,
barbara.franco@cima.fcen.uba.ar

Citation:

Franco, B. C., Palma, E. D., Combes, V., Acha, E. M., & Saraceno, M. (2018). Modeling the offshore export of Subantarctic Shelf Waters from the Patagonian shelf. *Journal of Geophysical Research: Oceans*, 123. <https://doi.org/10.1029/2018JC013824>

Received 23 JAN 2018

Accepted 29 MAY 2018

Accepted article online 14 JUN 2018

Modeling the Offshore Export of Subantarctic Shelf Waters From the Patagonian Shelf

B. C. Franco¹ , E. D. Palma^{2,3} , V. Combes⁴ , E. M. Acha^{5,6}, and M. Saraceno^{1,7} 

¹Centro de Investigaciones del Mar y la Atmósfera (CIMA)/CONICET-UBA, UMI-IFAECI/CNRS, Buenos Aires, Argentina,

²Departamento de Física, Universidad Nacional del Sur, Bahía Blanca, Argentina, ³Instituto Argentino de Oceanografía (IADO)

(CONICET-UNS), Bahía Blanca, Argentina, ⁴College of Earth, Ocean, and Atmospheric Sciences, Oregon State University, Corvallis,

OR, USA, ⁵Instituto Nacional de Investigación y Desarrollo Pesquero (INIDEP), Mar del Plata, Argentina, ⁶Instituto de

Investigaciones Marinas y Costeras (IIMyC) (CONICET-UNMdP), Mar del Plata, Argentina, ⁷Departamento de Ciencias de la

Atmósfera y los Océanos (DCAO), Facultad de Ciencias Exactas y Naturales, Universidad de Buenos Aires, Buenos Aires, Argentina

Abstract It has been suggested that the Subtropical Shelf Front (STSF) could be a preferential site for the detrainment of Subantarctic Shelf Water (SASW) and related planktonic shelf species onto the open SW Atlantic Ocean. The offshore detrainment of SASW and planktonic shelf species might be an exportation mechanism, affecting the population abundances of fishing resources in Argentina, Uruguay, and Southern Brazil. In this study, we characterize for the first time the 3-D structure of the STSF and the main routes of offshore export of SASW from the Patagonian shelf during austral summer (summer and early fall) and winter (winter and early spring) by using numerical hydrodynamical model results and Lagrangian tracking simulations of neutrally buoyant floats. The transport of SASW toward the open ocean is ~ 1 Sv ($1 \text{ Sv} = 10^6 \text{ m}^3/\text{s}$) during summer and ~ 0.8 Sv during winter. SASW are exported offshore mainly near the Brazil-Malvinas Confluence region during both seasons. The STSF appears to act as an important retention mechanism for the plankton over the inner and middle shelf mainly during late summer and early fall. Our findings could explain the life cycle of distinct fish species that are distributed in the region, as well as the population abundance variability of such species.

Plain Language Summary The Subtropical Shelf Front (STSF) has been suggested to be a preferential site for the detrainment of Subantarctic Shelf Water (SASW) from the Patagonian continental shelf toward the open ocean. This offshore detrainment of SASW might be an exportation mechanism to the open ocean of early larval stages of life of shelf fish species, affecting the population abundances of fishing resources in Argentina, Uruguay, and Southern Brazil. In this work we characterize the 3-D structure of the STSF, its dynamics and variability, and the main routes of offshore export of SASW during austral summer and winter for the first time. We discover that the main offshore detrainment of SASW occurs near the Brazil-Malvinas Confluence, while the STSF appears to act as an important retention mechanism for early larval stages of life of shelf fish species mainly during late summer and early fall. Our findings could explain the life cycle of distinct fish species that are distributed in the region, as well as the population variability of such species.

1. Introduction

In this article we discuss the detrainment of the Subantarctic Shelf Water (SASW) from the Patagonian shelf toward the neighboring deep ocean. Previous studies have suggested that the main detrainment of these shelf waters and planktonic shelf species onto the open ocean occur along a subsurface thermohaline front (the Subtropical Shelf Front [STSF]; Möller et al., 2008; Piola et al., 2000, 2008). These previous studies, based on synoptic hydrographic in situ observations, were able to characterize the temperature-salinity (T - S) signature of SASW over the shelf and in the deep ocean. However, these observations were not suitable in time and space to fully understand the 3-D structure of the STSF, neither to quantify the transport of SASW toward the open ocean throughout the frontal region. In this article we focus on the description and analysis of the STSF 3-D structure, its seasonal variability, and the main routes of offshore export of SASW from the Patagonian shelf by using the results of a numerical hydrodynamical model and Lagrangian tracking simulations using neutrally buoyant floats. This is a first approach that brings new insights to the understanding of the water circulation in this complex area and deals with important issues of the circulation of shelf waters in the SW Atlantic Ocean region and its relationship with the STSF, its structure, and the export of shelf waters to the open ocean.

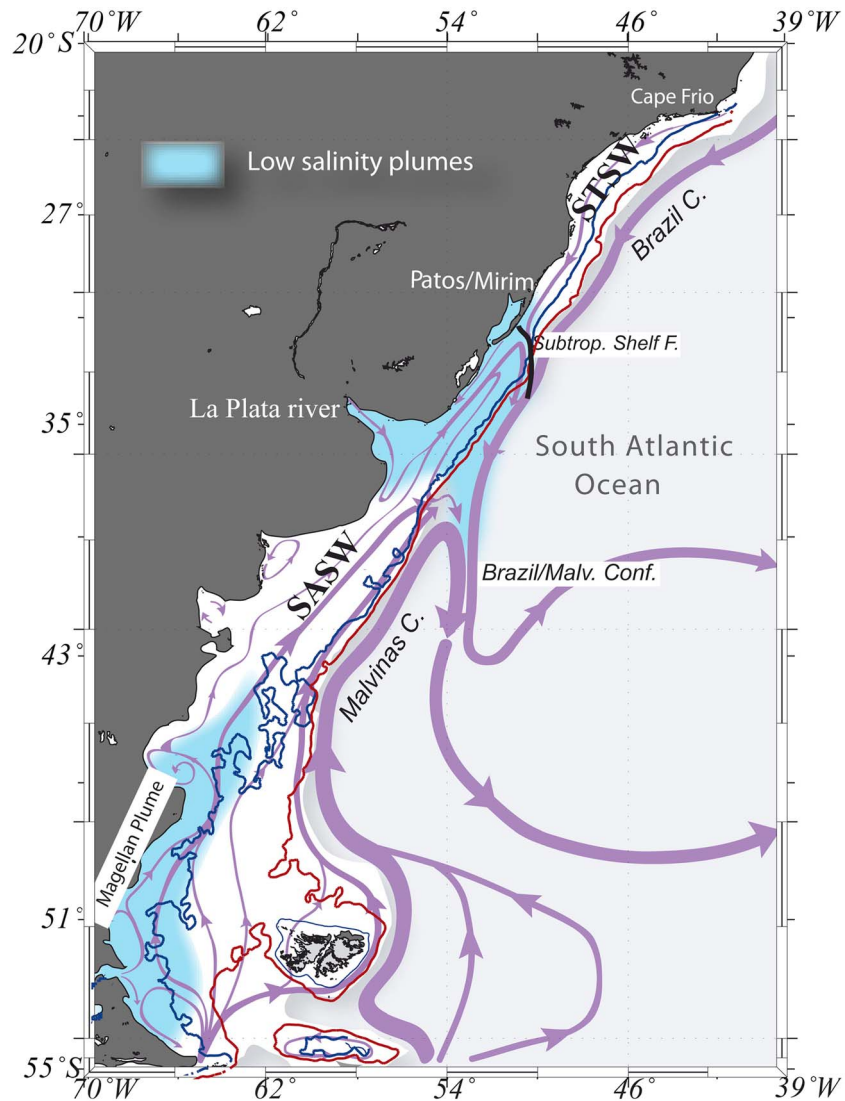


Figure 1. Schematic depiction of the circulation in the Southwestern Atlantic Shelf (SWAS). Subantarctic Shelf Waters (SASW); Subtropical Shelf Water (STSW). The black line represents the Subtropical Shelf Front. The blue color emanating from the Rio de la Plata, Patos/Mirim Lagoon, and the Strait of Magellan denotes sea surface salinity < 33.5 (adapted from Strub et al., 2015). The isobaths of 100 (blue) and 200 m (red) are shown.

1.1. Background

The Southwestern Atlantic Shelf extends from the tip of Tierra del Fuego (55°S), Argentina to Cabo Frío (~22°S), Brazil. This work focuses on the Central Shelf Region between approximately 40°S and 31°S (e.g., Palma et al., 2008), which is thought to be the portion of the Southwestern Atlantic Shelf where SASW leaks to the deep ocean. The hydrographic structure of this shelf region has been extensively described in previous studies (e.g., Bianchi et al., 2005; Guerrero & Piola, 1997; Piola et al., 2000, 2008). It is characterized mainly by two shelf water masses: SASW, a relatively fresh ($S < 34$) variety of subantarctic water that is injected onto the Patagonian shelf (55°S) through the Le Maire Strait, the shelf break indentation between Tierra del Fuego and Burdwood Bank and to less extent the Patagonian shelf break running north-south (i.e., Malvinas Current; Figure 1); and Subtropical Shelf Water (STSW), a more saline ($S > 35$) and warmer water composed of modified South Atlantic Central Water diluted by continental runoff from the coast of Brazil (Piola et al., 2000). These water masses reflect the dominant circulation patterns of the Central Shelf Region. Offshore, over the shelf break and slope, there is an influence of two distinctive western boundary currents: the Brazil and Malvinas currents (Figure 1).

The STSF comprises a transition region between STSW and SASW (Piola et al., 2000). The front is located near the 50-m isobath at 32°S over the inner shelf off Rio Grande, Brazil, and extends southward reaching the shelf break close to 36°S. The front acts like a barrier to the northward displacement of SASW and the southward displacement of STSW; it has been suggested consequently that the STSF could be a preferential site for the detrainment of shelf waters and related planktonic species onto the deep ocean (Matano et al., 2010; Piola et al., 2000, 2008). The STSF appears to be an extension over the continental shelf of the subantarctic-subtropical transition observed at the Brazil-Malvinas Confluence (BMC; Piola et al., 2000). The Malvinas Current may play an important role in the front location through its barotropic pressure gradient (Palma et al., 2008). The subsurface manifestation of the front is capped at the surface by a low salinity tongue generated by the discharge of the Rio de la Plata (RdIP) and the Patos/Mirim Lagoon (Piola et al., 2000). The major freshwater inflow into the shelf is associated with the RdIP discharge, which averages $\sim 23,300 \text{ m}^3/\text{s}$. A secondary freshwater discharge is from the Patos/Mirim Lagoon system, located near 32°S, averaging between 1,500 and 2,000 m^3/s (Möller, 1996; Möller et al., 1991). Both discharges create a freshwater plume (hereafter La Plata plume) that spreads along the coastlines of Argentina, Uruguay, and Brazil and into the deep ocean (Guerrero et al., 2014; Matano et al., 2014). Salinities lower than 33.4, found north of 36°S, require mixtures of RdIP and Patos/Mirim Lagoon waters. These low salinity waters ($S < 32.5$), referred as Plata Plume Water (PPW; e.g. Piola et al., 2008), fertilize the southern Brazilian shelf, making this area one of the most important fishing areas of this country (Castello et al., 1990).

North of $\sim 37^\circ\text{S}$, the flow direction and intensity over the shelf are relatively variable, in part due to a substantial decrease in the westerlies north of $\sim 40^\circ\text{S}$ and a relatively large seasonal component in the wind stress variability (Strub et al., 2015). The alongshelf extension of the La Plata plume varies with the seasons (Möller et al., 2008; Piola et al., 2008). Primarily in response to variations in the alongshore wind stress, the La Plata plume presents large northeastward penetrations along the continental shelf in late fall-winter, reaching as far north as 28°S (Piola et al., 2000). In contrast, in late spring-summer, the plume retracts southward until $\sim 32^\circ\text{S}$ and also spreads in the upstream direction (south of the RdIP outfall), extending nearly 300 km south of the mouth of the estuary (Framiñan et al., 1999; Guerrero et al., 1997; Piola et al., 2000). These seasonal La Plata plume variations induce a large impact on the shelf ecosystem (e.g., Castello et al., 1990; Ciotti et al., 1995; Muelbert & Sinque, 1996; Sunyé & Servain, 1998). Satellite-derived sea surface salinity (SSS) data indicate that in austral summer, mixtures of low salinity shelf waters are swiftly driven toward the ocean interior along the axis of the BMC (Guerrero et al., 2014). Their analysis shows that in summer, mixtures of low-salinity shelf waters from the RdIP expand to the outer shelf and are detrained from the shelf near 36°S–37°S. Similarly, simulated SSS fields show the detrainment of PPWs into the deep ocean near the BMC region (Matano et al., 2014). Altimeter sea surface height fields accurately capture the variability of the La Plata Plume along the continental shelf (Saraceno et al., 2014), and it reports that the transport of inner shelf waters to the deep ocean is strongest during summer, offshore, and to the southeast of the RdIP (Strub et al., 2015).

Our knowledge of the circulation patterns over this large shelf region is limited by the scarcity of direct observations. There are few documented descriptions of current meter time series over the continental shelf, each lasting only a few months or less (Castro & Miranda, 1998; Rivas, 1997; Zavialov et al., 2002). During the past years, current meter time series launched over cross-shelf transects lasted up to 18 months recording data. Near $\sim 40^\circ\text{S}$, two 1-year current meter series have shown that the dynamics of the currents over the shelf is dominated by the wind; the average of the currents follow the NNE direction as predicted by the models (M. Saraceno, personal communication, January 05, 2018). Circulation patterns over the shelf have been therefore indirectly inferred mainly from hydrographic observations (Lucas et al., 2005; Möller et al., 2008; Piola et al., 2000, 2008) and from regional-scale numerical simulations (Combes & Matano, 2014a; Matano et al., 2014; Mendonça et al., 2017; Palma, Matano, Piola, & Sitz, 2004; Palma, Matano, & Piola, 2004; Palma et al., 2008; Pereira, 1989; Simionato et al., 2001; Soares et al., 2007). Seasonal changes of the circulation over the outer shelf are greatly influenced by the contiguous western boundary currents and their confluence zone (Combes & Matano, 2014a; Matano et al., 2010). According to the latter authors, Patagonian surface shelf waters are exported offshore mainly in the BMC region.

The complementary works by Guerrero et al. (2014) and Matano et al. (2014) were aimed at studying the spatial and temporal variabilities of the water masses off the vicinity of the RdIP and the adjacent deep ocean in the Southwestern Atlantic Ocean. The authors have described the marked seasonality of the salinity at the

continental shelf in the study area as well as the exportation processes driving the continental shelf waters into the deep ocean. Matano et al. (2014) described that the exportation patterns of these waters are driven by both the western boundary current dynamics in the study region and the local winds. The patterns change from late winter (1) to summer (2) when, respectively, low-salinity waters associated to the RdIP are driven (1) southward from the shelf north of the BMC region to the open ocean and (2) are funneled more directly into the BMC.

It has been proposed that interannual fluctuations in abundance of various species of commercial interest with planktonic larvae (Argentine squid, anchovy, and Patagonian scallop) could be related with the offshore export of the larvae (Bakun & Csirke, 1998; Bakun & Parrish, 1991; Brunetti & Ivanovic, 1992). The deep ocean is an oligotrophic system from which the larvae would have no way to return to the shelf, constituting a population loss. The offshore detrainment of those planktonic larvae might affect the abundance of fishing stocks in Argentina, Uruguay, and Southern Brazil.

2. Material and Methods

2.1. Hydrodynamic Numerical Model

The Lagrangian particle tracking approach, explained in the following section, uses the outputs of a high-resolution ocean hydrodynamical model developed by Combes and Matano (2014a). The ocean model is based on the Regional Ocean Modeling System (ROMS_AGRIF version; Debreu et al., 2012), which is a three-dimensional, free surface, hydrostatic, eddy-resolving primitive equation ocean model. The model uses a high-resolution “child” grid embedded into a coarser-resolution “parent” grid. The parent grid encompasses the entire Southern Hemisphere. It has a spatial resolution of $1/4^\circ$ with 40 terrain-following vertical levels. The child domain extends from 82°W to 41°W and from 64°S to 20°S , with a spatial resolution of $1/12^\circ$ and 40 vertical levels. The bottom topography is a smoothed version of ETOPO1 ($1'$ resolution; e.g., Amante & Eakins, 2009), to prevent from horizontal pressure gradient errors (Beckmann & Haidvogel, 1993). At the northern boundary of the parent grid, the model is nudged to the monthly mean climatology provided by the OFES model (Masumoto et al., 2004). The OFES model also provides the initial condition. To spin-up the model, the parent configuration was first integrated during a 10-year period and then the parent/child configuration for an additional 15-year period. Several sensitivity experiments were carried out by the authors, and the results obtained by the EXP_SEASON were considered the most realistic for the child region. EXP_SEASON was forced at the surface with monthly mean climatological wind stress from ERA-Interim data corresponding to the period 1972–2012 (Dee et al., 2011) and heat and freshwater fluxes from the COADS data set (da Silva et al., 1994). The model forcing also includes a $23,000\text{ m}^3/\text{s}$ discharge from La Plata River and the principal semidiurnal tidal constituent (M_2). For vertical mixing, the model uses a K-Profile Parameterization scheme (Large et al., 1994) and a quadratic friction law with a friction parameter $\alpha = 0.045$. No explicit horizontal diffusion and viscosity have been added. More detailed technical description of the model configuration can be found in Combes and Matano (2014a). For the present study, we used a climatological average of the last 10 years of the model run.

2.2. Lagrangian Tracking Simulation

Diagnostic studies using neutrally buoyant floats were used to identify the offshore pathways taken by SASW from the Patagonian continental shelf. During their northward journey along the shelf, SASW are subject to intense mixing with PPW, STSW, and Tropical Water until their offshore export. To evaluate the impact of this mixing on salinity and temperature characteristics, we released neutrally buoyant floats along the continental shelf at 38°S and tracked their salinity and temperature variations as well as their depth and residence time. A number of 840 floats are evenly distributed in each model's sigma level (each grid element) at the beginning of the austral summer (JFM) and winter (JAS) and tracked during 135 days.

3. Results and Discussion

3.1. Characterization of the STSF

To characterize the STSF, we construct T - S and quantitative T - S diagrams employing the model's output data. The data were averaged for each season, and only subsurface data ($z < -50\text{ m}$) located between the 50 and 200 m isobath were used to construct the T - S diagrams. The thermohaline indexes used to describe the main

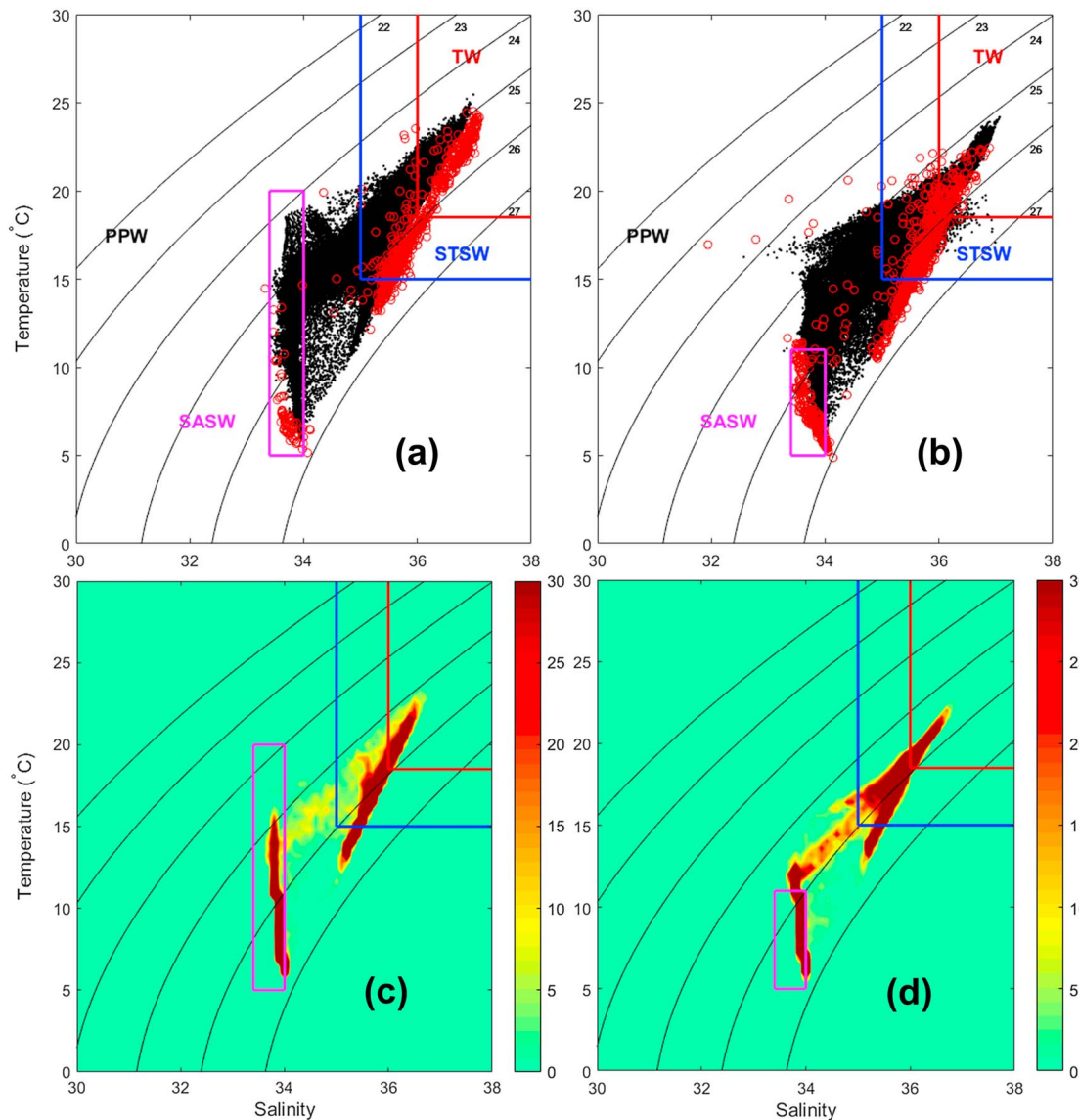


Figure 2. Temperature-salinity (T - S) diagrams for both summer (a) and winter (b) seasons and their respective quantitative T - S diagrams (c) and (d), respectively. Model outputs (black dots) and historical hydrographic data (red circles) from Piola et al. (2000) are shown for both seasons. To configure the T - S diagrams for the model outputs, only subsurface data ($z < -50$ m) located between the 50- and 200-m isobath were used. Historical hydrographic data were also limited by data, $z < -50$ m. T - S characteristic limits of Subantarctic Shelf Water (SASW), Subtropical Shelf Water (STSW), and Tropical Water (TW) are shown by heavy lines (e.g., Piola et al., 2000). Solid lines (black) represent sigma- T (σ_T). The T - S indexes used to describe the main shelf water masses (SASW and STSW) followed Piola et al. (2000). PPW = Plata Plume Water.

shelf water masses (SASW and STSW) seen in Figure 2 followed Piola et al. (2000). To validate the model output, we employed historical hydrographic data collected along the shelf ($z > -200$ m) between 20°S and 40°S and from 1960 to 1990 (Piola et al., 2000). This large database is likely to characterize climatological conditions, and therefore, we believe that is suitable for the validation of the model's performance in representing the STSF. T - S Diagrams for both the summer and winter seasons show that the model successfully represents the typical SASW and STSW masses and the STSF (Figures 2a and 2b). The STSF occurs along and extended alongshore region (~32°S–36°S) that is highly impacted by wind and freshwater discharges with pronounced seasonal and interannual variabilities (Matano et al., 2014; Piola et al., 2005), generating very distinct mixing processes. Our study is complemented with the characterization of the shelf processes exploring the T and S characteristics of the flow in different seasons using neutral floats.

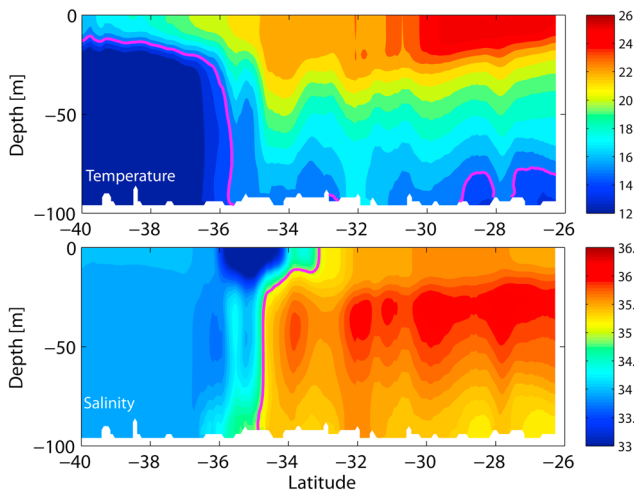


Figure 3. Temperature ($^{\circ}\text{C}$) and salinity (psu) vertical fields along the $\sim 100\text{-m}$ isobath during summer. The data represent an average for the austral summer (JFM) months. Subtropical Shelf Front (STSF) is characterized mainly by the isohaline of 35 (e.g., Piola et al., 2000). Typical T (15°C) and S (35) limits of STSF are shown by a magenta heavy isoline.

A comparison between the model results and observations indicates that the nested model has a skill in reproducing the best-known aspects of the regional circulation, for example, the volume transport of the Antarctic Circumpolar Current, the seasonal variability of the transport of the Malvinas and Brazil Currents, the latitudinal position of the BMC, the shelf break upwelling of Patagonia, and the Zapiola Anticyclone (Combes & Matano, 2014a). The seasonal changes of the Malvinas Current transport in the model are consistent with those inferred from satellite (AVISO Sea Surface Height) data, which shows similar seasonal differences in the geostrophic velocities between the austral winter and the austral summer. The regional patterns of the eddy kinetic energy in the model features the characteristic C-shape that extends from the BMC toward the southern limit of the Argentine basin in agreement with observations. The model's eddy kinetic energy intensity, however, appears higher than the observations in the deep ocean. The validation of this model was extended in several subsequent papers. Combes and Matano (2014b) studied the BMC location variability and its forcing mechanisms and compared the model results with satellite altimetry and SST. For the region of interest in our study, Matano et al. (2014) validated the model results of Combes and Matano (2014b) with satellite SSS (Aquarius) and in situ data. The comparison stresses the fact that a large part of SASW outflows near the BMC location.

Guerrero et al. (2014) extended the validation with an in-depth analysis of satellite and in situ SSS. Finally, the shelf circulation generated by the model between 43°S and 25°S is well correlated with the analysis of geostrophic currents derived from two independent studies using satellite altimetry (Saraceno et al., 2014; Strub et al., 2015).

The main observations about the accuracy of the model to represent the SASW in both seasons are that the values from the model are mostly saltier than the historical hydrographic data (Figures 2a and 2b). However, the comparison is pretty reasonable considering that most of SASW from the model's output data have $S < 34$. Temperature values for SASW are also very reasonable when comparing model and historical hydrographic data. Our quantitative T - S diagrams show the main presence of SASW and STSW over the shelf (Figures 2c and 2d). To construct the quantitative T - S diagrams from the model's output data, climatological seasonal means of T and S were extracted at each grid point along the shelf ($z > -200$ m) for depths

$z < -50$ m and between 20°S and 40°S , and the number of data for each interval of 0.4°C and 0.1 psu were recorded. Model outputs show a higher mixing between SASW and STSW during winter (Figures 2c and 2d). Historical hydrographic data also show a higher mixing between SASW and STSW during winter mainly between the σ_T isolines of 25 and 26 kg/m^3 . Observations from the historical hydrographic data show that intense cross-shelf mixing through isopycnal connections between SASW and STSW can occur in summer, due to the seasonal heating in surface layers ($z > -50$ m; e.g.; Piola et al., 2008). Such surface ($z > -50$ m) mixing processes cannot be observed from our model's output in the T - S diagrams.

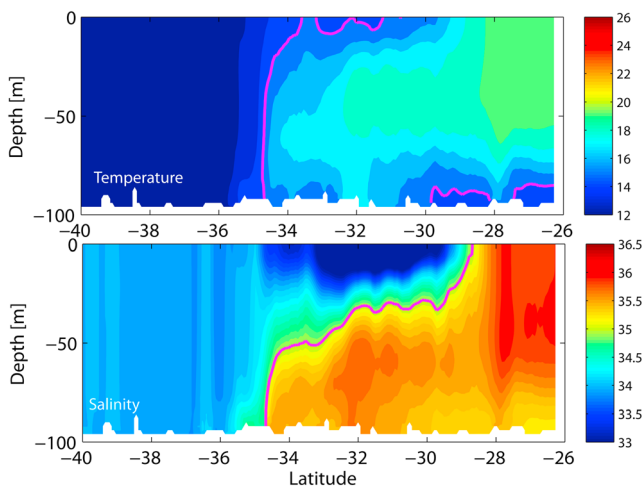


Figure 4. Temperature ($^{\circ}\text{C}$) and salinity (psu) vertical fields along the 100-m isobath during winter. The data represent an average for the austral winter (JAS) months. Subtropical Shelf Front (STSF) is characterized mainly by the isohaline of 35 (e.g., Piola et al., 2000). Typical T (15°C) and S (35) limits of STSF are shown by a magenta heavy isoline.

Temperature and salinity fields along the $\sim 100\text{-m}$ isobath reveal that the subsurface STSF is located mainly at about $\sim 35.5^{\circ}\text{S}$ – 35°S during austral summer (Figure 3). Mixing processes in the STSF are clearly shown by the salinity field. The STSF is characterized mainly by the isohaline of 35 (e.g., Piola et al., 2000). South of the frontal zone, SASW dominate the shelf, while STSW with $S > 35$ dominate the shelf north of $\sim 35^{\circ}\text{S}$.

During austral winter (Figure 4), the salinity vertical field reveals that the STSF is located approximately at the same latitude ($\sim 35.5^{\circ}\text{S}$). SASW with typical limits of temperature for winter ($T < 10$ – 12°C)

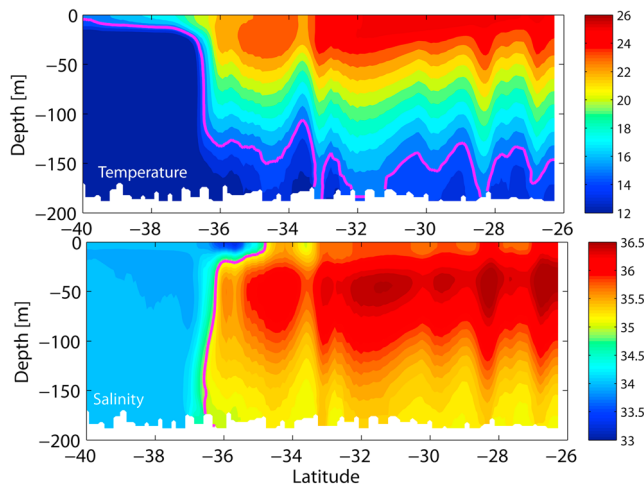


Figure 5. Temperature ($^{\circ}\text{C}$) and salinity (psu) vertical fields along the 200-m isobath during summer. The data represent an average for the austral summer (JFM) months. Subtropical Shelf Front (STSF) is characterized mainly by the isohaline of 35 (e.g., Piola et al., 2000). Typical T (15°C) and S (35) limits of STSF are shown by a magenta heavy isoline.

dominates the middle shelf mainly south of 36°S . The signature of PPW is clearly larger in winter than during summer. Waters with $S < 33.6$ spread until about 29°S in subsurface waters ($\sim 30\text{--}40$ m depth). A higher mixing between PPW and STSW is observed along the water column mainly between 30 and 40 m depth until regions where depths are < -60 m (Figure 4).

Temperature and salinity fields along the 200 m reveal the subsurface STSF located mainly about $\sim 37^{\circ}\text{S}\text{--}36^{\circ}\text{S}$ during austral summer (Figure 5). Waters saltier than 34 nearly $\sim 40^{\circ}\text{S}$ have been observed previously by Franco et al. (2017), who analyzed results of the same hydrodynamical model. Intrusions of Malvinas Current waters onto the continental shelf near $\sim 41^{\circ}\text{S}$ were previously reported (Piola et al., 2010). Their work suggests that the intrusions of cold, nutrient-rich waters of the current are important in promoting the local development of phytoplankton near 41°S . There is no standard definition to characterize the meridional position of the STSF, but based in the work of Piola et al. (2000), we decided to define the frontal position using the latitudinal location of the 35 isohaline at 60 m depth on the 100 isobath. Selecting the location of the maximum salinity gradient instead of the position of the 35 isohaline produced a similar latitudinal position for the STSF. Selecting a shallower position on the water column introduced large differences associated with the seasonal expansion and retraction of the La Plata plume. Using the climatological model results (i.e., the average over the full model run) and this definition, the front is sharp all year long (not shown). Ocean internal variability may generate different dynamical situations in different years of a long-term simulation. However, both model and observations (i.e., Piola et al., 2000, 2008) indicate a very robust location of the STSF. A time series of the STSF location constructed from data from an extended model simulation (1979–2012 forced with 3-day averaged fields from the ERA-Interim data set) (Combes & Matano, 2014b) indicates that both the seasonal and the interannual variabilities of the STSF location is less than 0.6° (not shown).

During austral winter, the salinity vertical field reveals that the STSF is located mainly about 36°S in subsurface waters (~ 80 m depth), while it is located at $\sim 37^{\circ}\text{S}$ in waters deeper than ~ 110 m. Higher mixing between SASW and STSW is observed mainly above ~ 110 m (Figure 6).

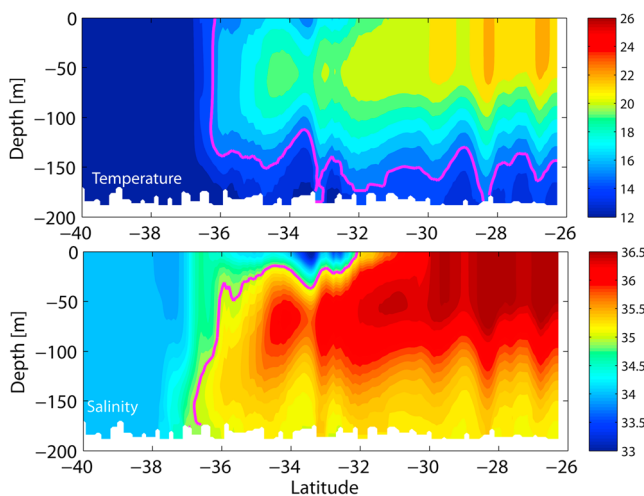


Figure 6. Temperature ($^{\circ}\text{C}$) and salinity (psu) vertical fields along the 200-m isobath during winter. The data represent an average for the austral winter (JAS) months. Subtropical Shelf Front (STSF) is characterized mainly by the isohaline of 35 (e.g., Piola et al., 2000). Typical T (15°C) and S (35) limits of STSF are shown by a magenta heavy isoline.

3.2. Shelf Transport

As a first estimation of the path of Patagonian shelf waters north of 38°S , we computed the latitudinal variation of the total (northward) transport from the coast until depths lower than 200 m. The main offshore detrainment of SASW (stronger decrease of the flow) occurs mainly south of $\sim 36.5^{\circ}\text{S}$ during the austral summer (Figure 7a) and south of $\sim 37^{\circ}\text{S}$ during the austral winter and its months (Figure 7b). During summer, northward flows over the continental shelf north of $\sim 36.5^{\circ}\text{S}$ are lower than 0.4 Sv, and during winter, these flows are lower than 0.6 Sv north of $\sim 37^{\circ}\text{S}$. Therefore, SASW flowing northward as part of the northern limb of the STSF are almost a residual flux. During summer, for instance, north of $\sim 35^{\circ}\text{S}$, the northward flow is lower than ~ 0.2 Sv, and then the flow of SASW, which could reach the northern limb of the STSF is significantly low compared to that reported south of $\sim 36.5^{\circ}\text{S}$. North of $\sim 35^{\circ}\text{S}$, the northward flow is larger during winter than during summer (~ 0.4 Sv). The increase of the northward flow over the continental shelf north of $\sim 35^{\circ}\text{S}$ during winter could not be related only to the northward displacement of the RdIP discharge (~ 0.02 Sv). Our results reveal that during winter, mainly during July, there is a larger northward flow of SASW. Nevertheless, the offshore export of SASW throughout the STSF is lower than the offshore detrainment that occurs at about $\sim 36.5\text{--}37^{\circ}\text{S}$.

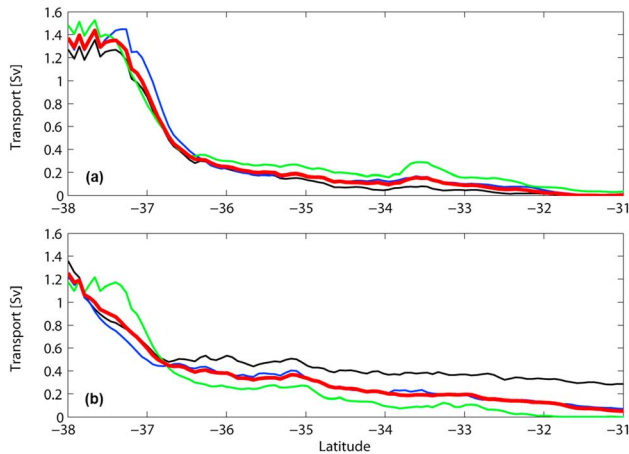


Figure 7. (a) Northward transport ($1 \text{ Sv} = 10^6 \text{ m}^3/\text{s}$) along the continental shelf from the coast until depths higher than -200 m averaged for the whole austral summer (heavy red line) and for each one of its months: January (black), February (blue), and March (green). (b) Northward transport (Sv) averaged for the whole austral winter (heavy red line) and for each one of its months: July (black), August (blue), and September (green).

Results recently reported by Mendonça et al. (2017) are in agreement with ours: they show a clear seasonal change in the volume of the STSF and the SASW seasonal variability in the offshore region.

3.3. Pathways of SASW

The offshore pathways taken by SASW from the continental shelf are examined diagnostically using neutrally buoyant floats (840) released at 38°S during early summer and winter. The floats were tracked during a period of 135 days and therefore are representative of the entire season that started at release time.

Most of the floats released over the middle and outer shelf in January are exported offshore mainly through the BMC until about 60 days, while the remaining floats proceed northward and drifts over the middle shelf for more than 100 days (April, early fall) (Figure 8a). Temperatures of surface and subsurface waters reported during the pathways of the floats are shown in Figure 8b. This analysis shows that higher values of temperature are reached by floats that are drifting over the surface coastal region and over the surface middle shelf. Pathways of SASW ($S < 34$) are observed alongshelf until the northern limb of the STSF in Figure 8c. Some floats move alongshore during

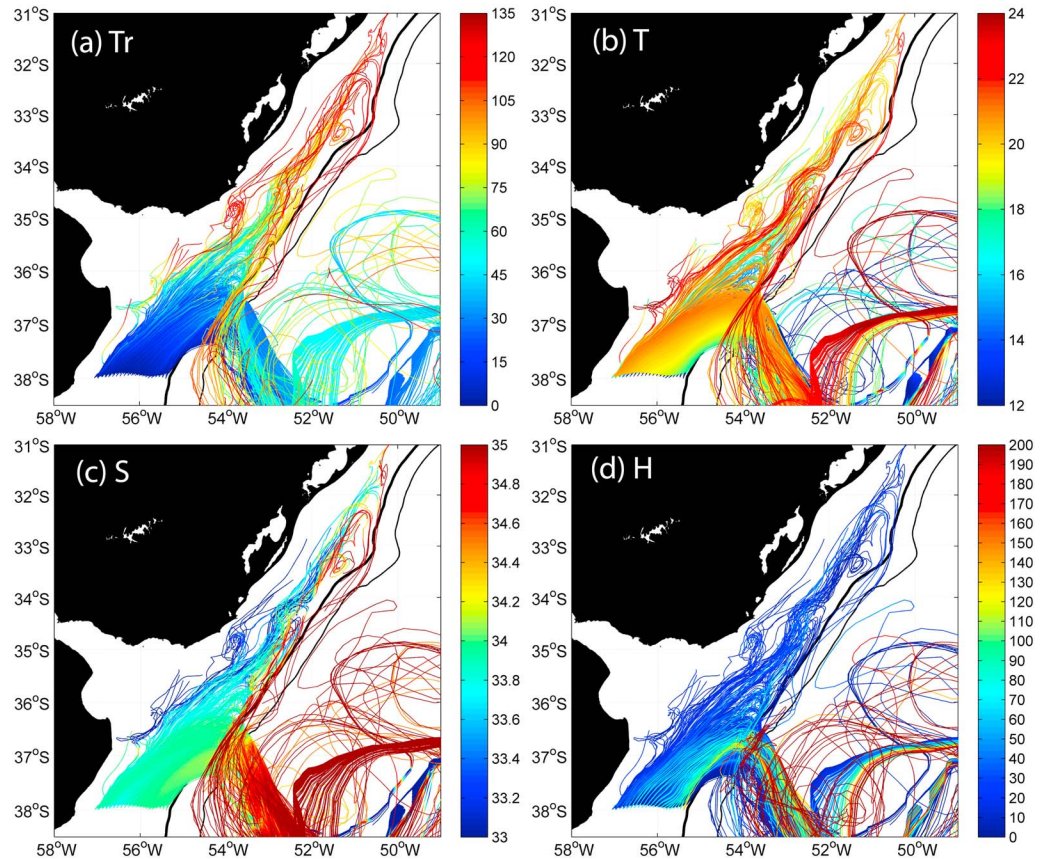


Figure 8. (a) Residence time (Tr), (b) temperature (T), (c) salinity (S), and (d) depth (H) of floats (840) distributed along the water column and released along the continental shelf at 38°S . Color bar indicates days from release in panel (a), T (degrees) in (b), S (psu) in (c), and H (m) in (d). Floats were tracked during a period of 135 days from 1 January to 15 May. The isobaths of 200 (heavy black line) and 1,000 m (thin black line) are shown.

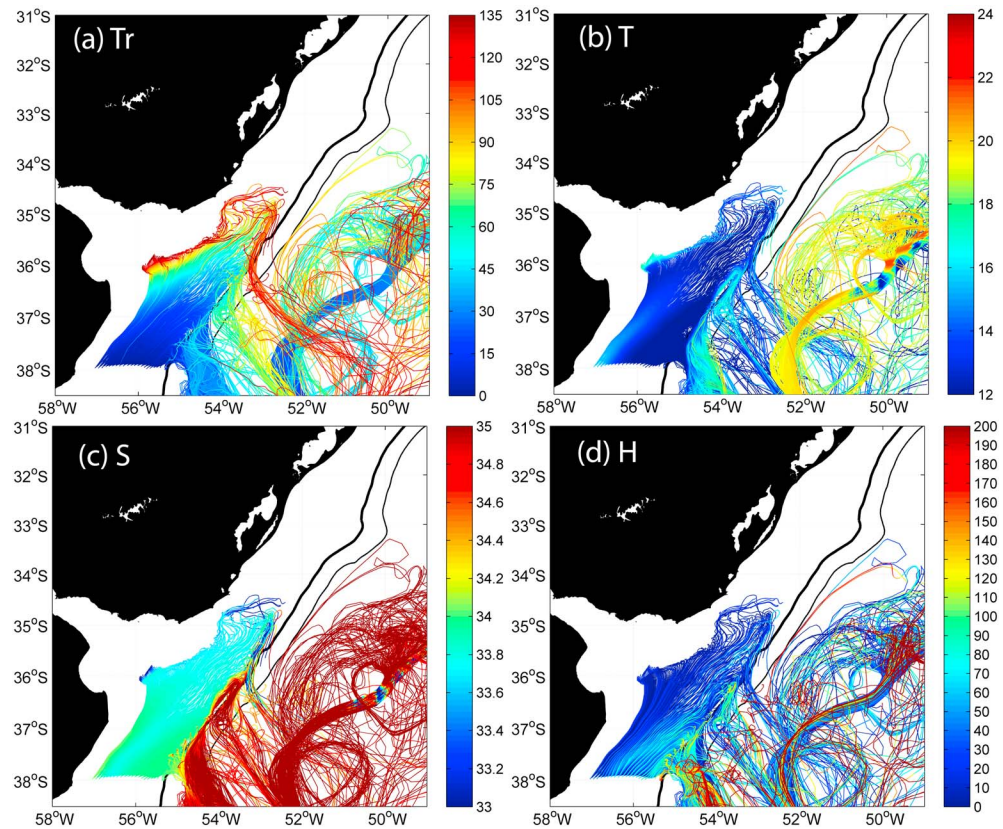


Figure 9. Idem as Figure 8 but for floats tracked from 1 July to 15 November. The isobaths of 200 (heavy black line) and 1,000 m (thin black line) are shown.

summer reaching higher values of salinity (through mixing processes with STSW), mainly when these floats reach the northern limb of the STSF (~32°S) over the middle-outer shelf and return toward the south over the outer shelf (early fall). The floats reach the northern limb of the STSF in middle April and at depths larger than 40 m (Figures 8a and 8d).

The floats released in July perform a northeastward trajectory during the first 60 days of simulation. By the end of the experiment, however, the floats that remain on the shelf show large residence times (>135 days, Figure 9a) with a possible retention mechanism between 36°S and 34.5°S close to the boundary of the RdIP plume at this time of the year (middle spring, November). The floats' behavior is related to the changes in the shelf circulation driven by the wind stress. During the first 60 days of simulation, the wind is mostly northwesterly north of 36°S, but it changes direction toward the southeast during spring (Piola et al., 2008). This change in wind direction induces a southward flow over the Southern Brazilian Shelf and a concomitant retraction of the edge of the RdIP plume (Guerrero et al., 2014; Matano et al., 2014; Piola et al., 2008). Some northeastward float's trajectories are observed during early spring along the coast of Uruguay and southern Brazil reaching ~35°S, while floats that reach ~34.5°S show a sharp decrease of salinity $S < 33$ and an increase in its temperature (see Figures 9b and 9c). Some floats reach the outer shelf while others are detrained offshore. It is interesting to note that the point of detrainment of shelf waters from the shelf is related to its residence time. The majority of the floats released in July are exported offshore near 37.5°S (Figure 9a), while the ones with larger residence times leave the shelf at two additional escape points, one at ~36.5°S and the other further north (~35.5°S) in spring (November; Figure 9a).

Pathways of SASW ($S < 33.8$) along the middle and outer shelf until the northern limb of the STSF (~35°S) are observed in Figure 9c. North of 36°S, our results suggest that during late winter, part of the SASW is retained over the inner and middle shelf, and mixing processes of the SASW with low salinity PPW are dominant in this region (Figures 9b and 9c). South of 36°S, it is possible to identify the two additional offshore detrainment

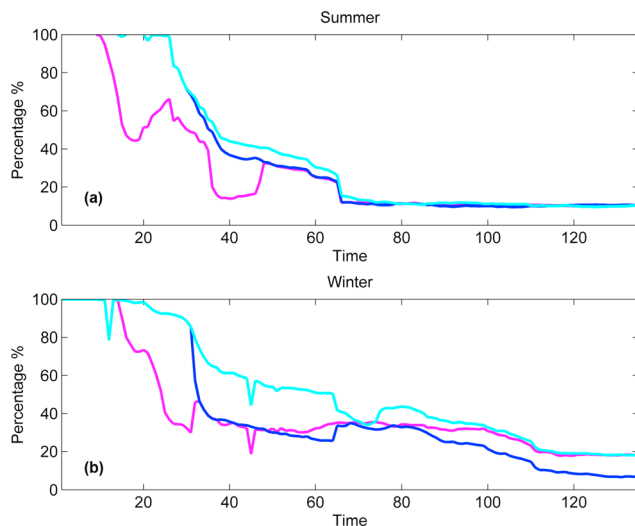


Figure 10. Percentage (%) of floats over the continental shelf ($z > -200$ m) during the (a) summer and (b) winter tracking simulation periods for each interval of latitude: 37°S – 36°S (magenta line), 36°S – 35°S (blue line), and 35°S – 34°S (cyan line).

routes of mixed SASW and saltier STSW toward the deep ocean (Figure 9c). These saltier waters are exported mainly in surface and subsurface waters (Figure 9d).

During summer and early march, the percentage of floats over the continental shelf ($z > -200$ m) located between 37°S and 36°S reaches about 40% in less than 20 days (Figure 10a). Our results indicate a very short time of residence for the offshore export of the floats. There are some fluctuations in the percentage along the days of tracking probably due to reversal (onshore) flows along the continental slope (M. Saraceno, personal communication); however, a percentage of floats lower than 20% over the shelf after 40 days of tracking indicates a great offshore export of SASW near the BMC. After ~ 65 days of tracking, less than 20% of the floats remain over the continental shelf between 36°S – 35°S and 35°S – 34°S . Our results show that the floats that follow alongshore over the middle shelf and reach the STSF by early fall are a low percentage of the initial released floats. During winter, the percentage of floats between 37°S – 36°S and 36°S – 35°S reaches about 40% in 30 and 35 days, respectively (Figure 10b). A higher percentage of floats between 35°S and 34°S during winter than during the summer is due to the large time of residence of the floats over the inner and middle shelf in late winter and early spring (see Figure 9).

4. Summary and Final Remarks

We characterize for the first time the 3-D structure of the STSF and the main routes of offshore export of SASW from the Patagonian shelf during austral summer (summer and early fall) and winter (winter and early spring) by using numerical hydrodynamical model results and Lagrangian tracking simulations of neutrally buoyant floats.

In summary, there are at least two routes of escape of SASW from the shelf, and the timescale of these two routes is very different. The main outflow point is located near the BMC, but the floats' trajectories indicates a fast timescale (less than 2 months), where most SASW is rapidly detrained offshore, and a slow timescale (>130 days), where a small portion of SASW surpass the BMC location and after a cyclonic loop turns back following the shelf break until the BMC. The second route however is only possible if the floats surpass the BMC location by the end of the summer (floats released from January to May). For floats released in winter (July to November), the second route is shorter and restricted to the mouth of the RdIP with several escape points to the deep ocean.

An additional computation of the offshore transport indicates that about 1 Sv of SASW is detrained toward the deep ocean by early fall at the BMC location. During late winter, this transport decreases to 0.8 Sv. These results are consistent with those reported in Matano et al. (2014). The low time of residence of the floats over the middle-outer shelf suggests that the offshore export of SASW and the intrusions of these fresher and colder waters in the open ocean north of the BMC mainly during winter highlight the role of the detrainment of SASW inducing shelf-deep ocean exchanges of salt and heat.

The STSF is not the preferential site for the detrainment of SASW from the Patagonian continental shelf toward the open ocean. However, the STSF appears to act as an important retention mechanism for the plankton over the inner and middle shelf mainly during late summer and early fall.

The model study reported in this study indicates that the offshore detrainment of SASW can induce mixing processes and heat and salt exchanges with waters from the Malvinas and Brazil Currents and might be an exportation mechanism to the deep ocean of planktonic larvae of shelf species, affecting the population abundances of fishing resources in Argentina, Uruguay, and Southern Brazil. Several commercial species evolved life cycles in which planktonic larvae exploit the high primary productivity of the shelf break, but at the same time, they are exposed to an offshore exportation to the oceanic realm becoming populational losses. Therefore, a better understanding about the dynamics of the BMC and the STSF including a dedicated field program together with dedicated model studies is required both to better estimate shelf-deep ocean

exchanges of salt and heat and also to manage resources in this heavily exploited area, with potential effects on biodiversity.

Acknowledgments

B.C.F. was supported by the Consejo Nacional de Investigaciones Científicas y Técnicas (CONICET) and Agencia Nacional de Promoción Científica y Tecnológica (ANCYP—grant PICT 2015-0508). E.D. Palma acknowledges the financial support from ANCYP (grant PICT16-0557) and Universidad Nacional del Sur (grant 24/F066). Support for V. Combes came from NASA grants (NNX17AH20G and NNX13AH22G) and National Science Foundation grants (OCE-1559550 and OCE-1357530). This research was also partially financed with the aid of a grant from the Inter-American Institute for Global Change Research (IAI) CRN 3070 (VOCES), which is supported by the National Science Foundation (grant GEO-1128040). All hydrographic data used in this study are available from the World Ocean Database at NOAA's National Center for Environmental Information (https://www.nodc.noaa.gov/OCS/WOD/pr_wod.html). The source code for the hydrodynamic model used in this study, ROMS_AGRIF, is freely available at https://www.croc-ocean.org/download/roms_agrif-project/. Comments from two anonymous referees are gratefully acknowledged.

References

- Amante, C., & Eakins, B. W. (2009). ETOPO1 1 arc-minute global relief model: Procedures, data sources and analysis. Technical Report NESDIS NGDC-24 (19 pp.). Washington, DC: National Geophysical Data Center, NOAA.
- Bakun, A., & Csirke, J. (1998). Environmental processes and recruitment variability. In P. G. Rodhouse, E. G. Dave, & R. K. O'Dor (Eds.), *Squid recruitment dynamics*, *FAO Fisheries Technical Paper* (Vol. 376, pp. 105–124).
- Bakun, A., & Parrish, R. H. (1991). Comparative studies of coastal pelagic fish reproductive habitats: The anchovy (*Engraulis anchoita*) of the southwestern Atlantic. *ICES Journal of Marine Science*, 48(3), 343–361. <https://doi.org/10.1093/icesjms/48.3.343>
- Beckmann, A., & Haidvogel, D. B. (1993). Numerical simulation of flow around a tall isolated seamount. Part I: Problem formulation and model accuracy. *Journal of Physical Oceanography*, 23(8), 1736–1753. [https://doi.org/10.1175/1520-0485\(1993\)023<1736:NSOFAA>2.0.CO;2](https://doi.org/10.1175/1520-0485(1993)023<1736:NSOFAA>2.0.CO;2)
- Bianchi, A. A., Bianucci, L., Piola, A. R., Pino, D. R., Schloss, I., Poisson, A., & Balestrini, C. F. (2005). Vertical stratification and air-sea CO₂ fluxes in the Patagonian shelf. *Journal of Geophysical Research*, 110, C07003. <https://doi.org/10.1029/2004JC002488>
- Brunetti, N. E., & Ivanovic, M. L. (1992). Distribution and abundance of early life stages of squid (*Illex argentinus*) in the south-west Atlantic. *ICES Journal of Marine Science*, 49(2), 175–183. <https://doi.org/10.1093/icesjms/49.2.175>
- Castello, J. P., Duarte, A. K., Möller, O. O., Niencheski, F., Odebrecht, C., Weiss, G., et al. (1990). On the importance of coastal and subantarctic waters for the shelf ecosystems off Rio Grande do Sul. Paper presented at II Simpósio de Ecossistemas da Costa Sul e Sudeste Brasileira: Estrutura, Função e Manejo. ACIESP (Vol. 74, pp. 112–119). São Paulo, Brazil.
- Castro, B. M., & Miranda, L. B. (1998). Physical oceanography of the western Atlantic continental shelf located between 4°N and 34°S. In A. R. Robinson, K. H. Brink (Eds.), *The Sea* (Vol. 11, chap. 8, pp. 209–251). New York: John Wiley.
- Ciotti, Á. M., Odebrecht, C., Fillmann, G., & Möller, O. O. (1995). Freshwater outflow and subtropical convergence influence on phytoplankton biomass on the southern Brazilian continental shelf. *Continental Shelf Research*, 15(14), 1737–1756. [https://doi.org/10.1016/0278-4343\(94\)00091-Z](https://doi.org/10.1016/0278-4343(94)00091-Z)
- Combes, V., & Matano, R. P. (2014a). A two-way nested simulation of the oceanic circulation in the southwestern Atlantic. *Journal of Geophysical Research: Oceans*, 119, 731–756. <https://doi.org/10.1002/2013JC009498>
- Combes, V., & Matano, R. P. (2014b). Trends in the Brazil/Malvinas Confluence region. *Geophysical Research Letters*, 41, 8971–8977. <https://doi.org/10.1002/2014GL02523>
- Debreu, L., Marchesiello, P., Penven, P., & Cambon, G. (2012). Two-way nesting in split-explicit ocean models: Algorithms, implementation and validation. *Ocean Modelling*, 49, 1–21. <https://doi.org/10.1016/j.ocemod.2012.03.003>
- Dee, D. P., Uppala, S. M., Simmons, A. J., Berrisford, P., Poli, P., Kobayashi, S., et al. (2011). The ERA-Interim reanalysis: Configuration and performance of the data assimilation system. *Quarterly Journal of the Royal Meteorological Society*, 137(656), 553–597. <https://doi.org/10.1002/qj.828>
- Framiñan, M. B., Etala, M. P., Acha, E. M., Guerrero, R. A., Lasta, C. A., & Brown, O. B. (1999). Physical characteristics and processes of the Rio de la Plata estuary. In G. Perillo, M. Piccolo, & M. Pino-Quivira (Eds.), *Estuaries of South America* (pp. 161–194). Springer: New York. https://doi.org/10.1007/978-3-642-60131-6_8
- Franco, B. C., Palma, E. D., Combes, V., & Lasta, M. L. (2017). Physical processes controlling passive larval transport at the Patagonian Shelf Break Front. *Journal of Sea Research*, 124, 17–25. <https://doi.org/10.1016/j.seares.2017.04.012>
- Guerrero, R. A., Acha, E. M., Framiñan, M. B., & Lasta, C. A. (1997). Physical oceanography of the Rio de la Plata Estuary, Argentina. *Continental Shelf Research*, 17(7), 727–742. [https://doi.org/10.1016/S0278-4343\(96\)00061-1](https://doi.org/10.1016/S0278-4343(96)00061-1)
- Guerrero, R. A., & Piola, A. R. (1997). Water masses in the continental shelf. In E. Boschi (Ed.), *The Argentine Sea and its fisheries resources* (Vol. 1, pp. 107–119). Mar del Plata: INIDEP.
- Guerrero, R. A., Piola, A. R., Fenco, H., Matano, R. P., Combes, V., Chao, Y., et al. (2014). The salinity signature of the cross-shelf exchanges in the southwestern Atlantic Ocean: Satellite observations. *Journal of Geophysical Research: Oceans*, 119, 7794–7810. <https://doi.org/10.1002/2014JC010113>
- Large, W. G., McWilliams, J. C., & Doney, S. C. (1994). Oceanic vertical mixing: A review and a model with a nonlocal boundary layer parameterization. *Reviews of Geophysics*, 32(4), 363–403. <https://doi.org/10.1029/94RG01872>
- Lucas, A. J., Guerrero, R. A., Mianzán, H. W., Acha, E. M., & Lasta, C. A. (2005). Coastal oceanographic regimes of the northern Argentine continental shelf (34°–43°S). *Estuarine, Coastal and Shelf Science*, 65(3), 405–420. <https://doi.org/10.1016/j.ecss.2005.06.015>
- Masumoto, Y., Sasaki, H., Kagimoto, T., Komori, N., Ishida, A., Sasai, Y., et al. (2004). A fifty-year eddy-resolving simulation of the world ocean: Preliminary outcomes of OFES (OGCM for the Earth Simulator). *Journal of Earth Simulator*, 1, 35–56.
- Matano, R. P., Combes, V., Piola, A. R., Guerrero, R., Palma, E. D., Strub, T. P., et al. (2014). The salinity signature of the cross-shelf exchanges in the southwestern Atlantic Ocean: Numerical simulations. *Journal of Geophysical Research: Oceans*, 119, 7949–7968. <https://doi.org/10.1002/2014JC010116>
- Matano, R., Palma, E. D., & Piola, A. R. (2010). The influence of the Brazil and Malvinas currents on the Southwestern Atlantic Shelf circulation. *Ocean Science*, 6(4), 983–995. <https://doi.org/10.5194/os-6-983-2010>
- Mendonça, L. F., Souza, R. B., Aseff, C. R. C., Pezzi, L. P., Möller, O. O., & Alves, R. C. M. (2017). Regional modeling of the water masses and circulation annual variability at the Southern Brazilian Continental Shelf. *Journal of Geophysical Research: Oceans*, 122, 1232–1253. <https://doi.org/10.1002/2016JC011780>
- Möller, O. O. (1996). Hydrodynamique de La Lagune dos Patos: Mesures et modélisation, (Doctoral dissertation). Bordeaux, Nouvelle-Aquitaine: Université Bordeaux I.
- Möller, O. O., Paim, P. S. G., & Soares, I. D. (1991). Facteurs et mécanismes de la circulation des eaux dans l'estuaire de la Lagune dos Patos (RS, Brasil). *Bulletim Institute de Geologie du Bassin d'Aquitaine*, 49, 15–21.
- Möller, O. O., Piola, A. R., Freitas, A. C., & Campos, E. J. D. (2008). The effects of river discharge and seasonal winds on the shelf off southeastern South America. *Continental Shelf Research*, 28(13), 1607–1624. <https://doi.org/10.1016/j.csr.2008.03.012>
- Muelbert, J. H., & Sinque, C. (1996). Distribution of bluefish (*Pomatomus saltatrix*) larvae along the continental shelf off southern Brazil. *Marine and Freshwater Research*, 47(2), 311–314. <https://doi.org/10.1071/MF9960311>
- Palma, E. D., Matano, R. P., & Piola, A. R. (2004). A numerical study of the Southwestern Atlantic Shelf circulation: Barotropic response to tidal and wind forcing. *Journal of Geophysical Research*, 109, C08014. <https://doi.org/10.1029/2004JC002315>
- Palma, E. D., Matano, R. P., & Piola, A. R. (2008). A numerical study of the Southwestern Atlantic Shelf circulation: Stratified ocean response to local and offshore forcing. *Journal of Geophysical Research*, 113, C11010. <https://doi.org/10.1029/2007JC004720>

- Palma, E. D., Matano, R. P., Piola, A. R., & Sitz, L. E. (2004). A comparison of the circulation patterns over the southwestern Atlantic Shelf driven by different wind stress climatologies. *Geophysical Research Letters*, *31*, L24303. <https://doi.org/10.1029/2004GL021068>
- Pereira, C. S. (1989). Seasonal variability in the coastal circulation on the Brazilian continental shelf (29°S–35°S). *Continental Shelf Research*, *9*(3), 285–299. [https://doi.org/10.1016/0278-4343\(89\)90029-0](https://doi.org/10.1016/0278-4343(89)90029-0)
- Piola, A. R., Avellaneda, N. M., Guerrero, R. A., Jardón, F. P., Palma, E. D., & Romero, S. I. (2010). Malvinas-slope water intrusions on the northern Patagonia continental shelf. *Ocean Science*, *6*(1), 345–359. <https://doi.org/10.5194/os-6-345-2010>
- Piola, A. R., Campos, E. J., Möller, O. O., Charo, M., & Martínez, C. (2000). Subtropical Shelf Front off eastern South America. *Journal of Geophysical Research: Oceans*, *105*(C3), 6565–6578. <https://doi.org/10.1029/1999JC000300>
- Piola, A. R., Matano, R. P., Palma, E. D., Möller, O. O., & Campos, E. J. (2005). The influence of the Plata River discharge on the western South Atlantic shelf. *Geophysical Research Letters*, *32*, L01603. <https://doi.org/10.1029/2004GL021638>
- Piola, A. R., Möller, O. O., Guerrero, R. A., & Campos, E. J. (2008). Variability of the Subtropical Shelf Front off eastern South America: Winter 2003 and summer 2004. *Continental Shelf Research*, *28*(13), 1639–1648. <https://doi.org/10.1016/j.csr.2008.03.013>
- Rivas, A. L. (1997). Current meter observations in the Argentine continental shelf. *Continental Shelf Research*, *17*(4), 391–406. [https://doi.org/10.1016/S0278-4343\(96\)00039-8](https://doi.org/10.1016/S0278-4343(96)00039-8)
- Saraceno, M., Simionato, C. G., & Ruiz-Etcheverry, L. A. (2014). Sea surface height trend and variability at seasonal and interannual time scales in the southeastern South American continental shelf between 27°S and 40°S. *Continental Shelf Research*, *91*, 82–94. <https://doi.org/10.1016/j.csr.2014.09.002>
- da Silva, A. M., Young, C. C., & Levitus, S. (1994). *Atlas of surface marine data 1994, Vol. 1: Algorithms and procedures, NOAA Atlas NESDIS (Vol. 8, p. 83)*. Washington, DC: U.S. Department of Commerce, NOAA, NESDIS.
- Simionato, C. G., Nuñez, M. N., & Engel, M. (2001). The salinity front of the Río de la Plata—A numerical case study for winter and summer conditions. *Geophysical Research Letters*, *28*(13), 2641–2644. <https://doi.org/10.1029/2000GL012478>
- Soares, I. D., Kourafalou, V., & Lee, T. N. (2007). Circulation on the western South Atlantic continental shelf: 2. Spring and autumn realistic simulations. *Journal of Geophysical Research*, *112*, C04003. <https://doi.org/10.1029/2006JC003620>
- Strub, P. T., James, C., Combes, V., Matano, R. P., Piola, A. R., Palma, E. D., et al. (2015). Altimeter-derived seasonal circulation on the southwest Atlantic shelf: 27°–43°S. *Journal of Geophysical Research: Oceans*, *120*, 3391–3418. <https://doi.org/10.1002/2015JC010769>
- Sunyé, P. S., & Servain, J. (1998). Effects of seasonal variations in meteorology and oceanography on the Brazilian sardine fishery. *Fisheries Oceanography*, *7*(2), 89–100. <https://doi.org/10.1046/j.1365-2419.1998.00055.x>
- Zavialov, P., Möller, O. O., & Campos, E. J. D. (2002). First direct measurements of currents on the continental shelf of southern Brazil. *Continental Shelf Research*, *22*(14), 1975–1986. [https://doi.org/10.1016/S0278-4343\(02\)00049-3](https://doi.org/10.1016/S0278-4343(02)00049-3)